AGU ADVANCING EARTH AND SPACE SCIENCE

Water Resources Research

RESEARCH ARTICLE
10.1029/2020WR027951

**Key Points:**
- We observed an increase in methylmercury concentrations but stable total mercury concentrations along a hydroelectric reservoirs sequence
- Methylmercury was linked to carbon dioxide, peaking in spring, consistent with accumulation and production in the winter under ice cover
- Methylmercury patterns were linked to signs of organic matter processing occurring months prior, and kilometers upstream

**Supporting Information:**
- Supporting Information S1

**Correspondence to:**
J. De Bonville and J.-F. Lapierre,
jeremy.de.bonville@umontreal.ca;
jean-francois.lapierre.1@umontreal.ca

**Citation:**
De Bonville, J., Amyot, M., del Giorgio, P., Tremblay, A., Bilodeau, F., Ponton, D. E., & Lapierre, J.-F. (2020). Mobilization and transformation of mercury across a dammed Boreal River are linked to carbon processing and hydrology. *Water Resources Research*, *56*, e2020WR027951. https://doi.org/10.1029/2020WR027951

Received 14 MAY 2020
Accepted 18 SEP 2020
Accepted article online 22 SEP 2020



# Mobilization and Transformation of Mercury Across a Dammed Boreal River Are Linked to Carbon Processing and Hydrology

**Jeremy De Bonville[1], Marc Amyot[1], Paul del Giorgio[2], Alain Tremblay[3], François Bilodeau[3], Dominic E. Ponton[1], and Jean-François Lapierre[1]**

[1]Groupe Interuniversitaire en Limnologie et en Environnement Aquatique (GRIL), Département de Sciences Biologiques, Université de Montréal, Montréal, Quebec, Canada, [2]Groupe Interuniversitaire en Limnologie et en Environnement Aquatique (GRIL), Département des Sciences Biologiques, Université du Québec à Montréal, Montréal, Quebec, Canada, [3]Hydro-Québec, Unité Expertise-Environnement Naturel et Humain, Montréal, Quebec, Canada

**Abstract** Reservoirs are known to accelerate the mobilization and cycling of mercury and carbon as a result of flooding of terrestrial organic matter, which can lead to environmental concerns at local and broader spatial scales. We explored the covariation of mercury (Hg) and carbon (C) functional pools in natural and recently dammed portions of the aquatic network of the Romaine River watershed in Northern Quebec, Canada, to understand how the fate of these elements varies across systems with contrasting hydrology and environmental conditions. We found that total Hg (THg) concentrations in surface waters were relatively constant along the network, whereas both the concentrations and proportions of MeHg tended to increase in reservoirs compared to surrounding nonflooded systems, and along the cascade of reservoirs. Whereas THg was related to total and terrestrial pools of dissolved organic carbon (DOC), MeHg was weakly related to DOC but strongly linked to surface concentrations of $CO_2$, as well as to concentrations of iron and manganese. The latter are proxies of cumulative organic matter processing within the network, presumably in anoxic portions of shallow bays, deep reservoir waters, and river sediments, as well as in prior seasons (e.g., under ice). Our results suggest that these deep boreal reservoirs acted more as transformation sites for Hg that was already present than as mobilizers of new Hg, and that under ice metabolism plays a role in MeHg production in these systems as we found strong dichotomies in MeHg patterns between spring and summer.

## 1. Introduction

Over 30,000 dams have been built over the past half-century, affecting nearly 20% of the global annual runoff from rivers (Zhou et al., 2015) and over 60% of rivers longer than 1,000 km (Grill et al., 2019). The flooding of soil following dam construction is associated with environmental issues such as the transformation of mercury (Hg) into the neurotoxin methylmercury (MeHg) as well as an increase in carbon processing and subsequent greenhouse gas (GHG) emissions, which result from the remobilization and degradation of terrestrial organic matter (OM) (Mucci et al., 2008; Teodoru et al., 2012; Wang & Zhang, 2013). Globally, rivers export about 27 ± 13 Mmol $a^{-1}$ of Hg (Amos et al., 2014), with recent increases observed in the Northern Pacific from Asian watersheds where a large percentage of rivers have been impounded (Lehner et al., 2011), and where enhanced Hg outputs from reservoirs also have a potential impact on downstream fish mercury levels (Anderson, 2011; Kasper et al., 2014; Li et al., 2017; Mason et al., 1994). Thus, increasing damming activity could enhance mercury and carbon fluxes globally, but the role of reservoirs as either sources of new mercury versus reactors for the methylation of mercury already present in the network, as well as potential links between the mercury and carbon cycles, remains unclear in these transformed systems.

Impounding a river causes a shift from a lotic system to one sharing more similarities with a lentic system, modifying most environmental variables from the ecosystem. In particular, the reduction of the natural flow of the river favors particle settling and accumulation of sediments, diminishes turbidity and increases light penetration in the water column, affecting primary production and nutrient cycling (Wüest, 2002). Furthermore, river impoundment may stimulate different microbial pathways compared to predammed

conditions, by providing novel anoxic environments and promoting inputs of fresh OM from flooded soils, which can then be degraded in the water (Bravo et al., 2010; Gilmour & Henry, 1991; Hall et al., 2005). Damming also leads to an increase in sedimentation rates (Poff & Hart, 2002), which can trap Hg from the water column and potentially stimulate Hg transformation by sediment microbial communities (Bravo et al., 2010; Hall et al., 2005). Some of the key environmental factors that control Hg methylation, including lower pH, warmer water temperatures, and nutrient availability and the redox state of waters and sediments (Ullrich et al., 2001), may be enhanced following flooding (Wüest, 2002). Hence, inorganic mercury (Hg (II)) that was previously stored in soils and sediments may be transferred to the aquatic environment, where it can be methylated by different microorganisms including methanogens, and iron and sulfate-reducing bacteria (Bravo, Peura, et al., 2018; Compeau & Bartha, 1985; Fleming et al., 2006; Hamelin et al., 2011). It has also been shown that fluxes of other metals, such as iron (Fe) and manganese (Mn) at the sediment-water interface peaked under suboxic or anoxic conditions (Pakhomova et al., 2007), were positively related to Hg and MeHg mobilization in lakes (Chadwick et al., 2006) and that Mn and MeHg cycles were correlated in a hypereutrophic reservoir (Beutel et al., 2020). Furthermore, river Hg concentrations have been previously shown to correlate with Mn and Fe concentrations (Quémerais et al., 1998). This suggests that the redox conditions promoting Mn and Fe fluxes from the sediments to the water column may also promote the release of MeHg.

Damming affects C cycling through different biogeochemical pathways. Flooding of soils and terrestrial vegetation results in the remobilization of large amounts of OM and its biological and photochemical degradation, leading to the emission of $CO_2$ and $CH_4$ to the atmosphere (Teodoru et al., 2012), and the increased export of DOC downstream (Dalzell et al., 2005; Majidzadeh et al., 2017). Research conducted on reservoirs have shown that following flooding, the system may switch from being a C sink to a source, concurrent with increases of MeHg exports up to several orders of magnitude with effects lasting up to three decades (Kelly et al., 1997; Li et al., 2013). Recent studies have further demonstrated a link between dissolved OM (DOM) composition and the formation of MeHg, where the availability of microbial- and algal-derived DOM was associated with higher methylation rates within the system, and hence to higher MeHg concentrations (Bravo et al., 2017; Herrero Ortega et al., 2018). Total mercury (THg) concentrations, on the other hand, have been shown to be mostly associated with terrestrially derived DOM inputs, likely due to the tendency of Hg to bind to sulfur sites of DOC therefore travel together (Bravo, Kothawala, et al., 2018; Grigal, 2002). As a whole, current evidence suggests that flooding may concurrently alter biogeochemical transformations of Hg and C.

At the watershed level, hydrological pathways, water retention times, and timing of peak discharge may affect Hg dynamics in reservoirs, because altering the established river continuum with damming creates new conditions in terms of water chemistry, flow, and thermal regime (McCartney, 2009). In most freshwater systems, much of the Hg dynamics depend on local processing and environmental conditions that vary between different systems (Celo et al., 2006; Paranjape & Hall, 2017; Ullrich et al., 2001). However, concentrations of MeHg have been shown to increase across a series of connected reservoirs, driven by longer local residence times and the presence of anoxic hypolimnia (Zhao et al., 2017), whereas THg tends to remain stable or even decrease due to sedimentation that counterbalances new inputs (Bravo et al., 2010; Jiang et al., 2005). Therefore, in reservoir complexes built in a cascade configuration as a series of multiple reservoirs, Hg and C concentrations and composition at any given site does not only depend on environmental conditions in the immediate surroundings, but also on processes occurring upstream and over weeks to months prior.

In cold climates, rivers and reservoirs may be covered by ice during the winter, preventing exchanges between water and the atmosphere. In such conditions, OM processing in the water column and in the sediments may deplete oxygen in the water, leading to conditions suitable for Hg methylation and methanogenesis. For example, the few studies that have explored microbial activity under ice in lakes have found significant carbon processing, leading to an accumulation of $CO_2$ and $CH_4$ that is significant for yearly carbon budgets (Denfeld et al., 2018; Ducharme-Riel et al., 2015). Likewise, anoxic conditions at the sediment-water interface as well as in the water column have been shown to promote MeHg fluxes from the sediments to the water column in lakes (Feyte et al., 2012). Therefore, isolating the water column from the atmosphere through seasonal ice cover may represent an additional pathway leading to anoxic Hg and C processing, independent of the damming effect per se.

In this context, our main goals were to (1) understand the environmental and hydrological controls on Hg (MeHg and THg) distribution over a fluvial network that has been recently dammed and to (2) link Hg and organic carbon dynamics to proxies of carbon processing along this fluvial continuum, to ultimately (3) better understand the relative importance of within-reservoir versus surrounding landscape and upstream processes on Hg dynamics in the system. To do so, we applied a whole network approach to compare flooded and nonflooded systems, including lakes, rivers, and groundwaters in the catchment of a recently dammed boreal river.

## 2. Materials and Methods

### 2.1. Study Sites and Sampling Period

Our study was conducted in the Romaine River watershed in the boreal region of Quebec, Canada (50.3°N, 63.8°W). Since 2009, the river hydrology has been altered by the construction of four hydroelectric dams, which have been flooded in the following sequence: Romaine-2 (R2; 2014), Romaine-1 (R1; 2015), and Romaine-3 (R3; 2017). The last one, Romaine-4 (R4), is planned for 2020. The river is approximately 450 km long and its total catchment area is 14,470 $km^2$. For most of its length, it flows partially confined within steep valley walls reaching 300 m above valley bottom, limiting the flooded area compared to other reservoirs in similar climate. Upon completion and at maximum capacity, the total reservoir area will be 279 $km^2$, accounting for less than 2% of the total watershed area (Hydro-Québec, 2018). Mean annual temperature (MAT) in the area is 1°C and mean annual precipitations (MAPs) is 1,030 mm in its southern portion, closer to sea, whereas in the northern portion of the river MAT is −3°C and MAP is 852 mm (30 year averages, data publicly available at Environment Canada). In 2017, the Romaine flowed into the St. Lawrence River estuary with a mean annual flow of 353 $m^3\ s^{-1}$ with values over 1,000 $m^3\ s^{-1}$ during spring melt, usually occurring in May, and presented a few irregular peaks in flow values in the winter due to energy demand and production (Hydro-Québec, 2018).

We repeatedly sampled between 50 and 80 sites in a sequence of three reservoirs as well as tributaries, lakes, groundwater, and the upstream and downstream portions of the river to compare natural, undisturbed sites with those located in a flooded area (Figure 1) in June 2017 and August 2016–2018. We focused our reservoir sampling on R2 and R1 because at the time of sampling there were large amounts of floating trees in R3 that limited accessibility. The R4 reservoir had not yet been flooded and is considered as the upstream river (UR) sites. Reservoir sites can be grouped into two types: (1) bays, corresponding to flooded valley bottoms where the water column is shallower, with soil rather than sediment at the bottom, and (2) the main channel, which is deeper and associated with a lower water residence time due to higher flow velocity of the river.

### 2.2. Sampling

Most reservoir samples were taken from a nonmetallic Zodiac boat. Water was collected 30 cm below the surface using Teflon tubing attached to a peristaltic pump. Prior to sample collection, the tubing was washed by flushing dissolved hydrochloric acid (10% volume/volume, v/v), Milli-Q water, and site water for at least 2 min. Water samples were collected as duplicates using an in-line Whatman 0.45 μm filtration capsule attached to the tubing for filtered samples. Plastic piezometers were sampled using a peristaltic pump with Teflon tubing for groundwater sampling. The sites in the upper portion of R2 reservoir, and all upstream river and lake sites were sampled using a hydroplane. Grab samples were taken in the upstream direction to avoid any metal contamination from the plane floats or fuel. We followed the clean hands, dirty hands sampling protocol to avoid any contamination by trace metals (St. Louis et al., 1994). Grab samples were filtered in the lab on a 0.45 μm polycarbonate membrane mounted on an acid (10% HCl) washed Teflon filtration tower on the same day. The tower was rinsed with HCl (10%) and MilliQ water between each site. In all cases, field and lab blanks were taken to identify potential contamination; blanks were consistently below the detection limit (0.01 ng $L^{-1}$) for MeHg. Following collection and filtration, samples were preserved in the lab using ultrapure hydrochloric acid to reach a 0.4% (v/v) final concentration and kept in the dark in a 4°C refrigerator for subsequent analysis.

Following the same protocol, we collected samples for total phosphorus (TP) and nitrogen (TN) as well as filtered water for dissolved organic carbon (DOC) and colored and fluorescent dissolved OM (CDOM and

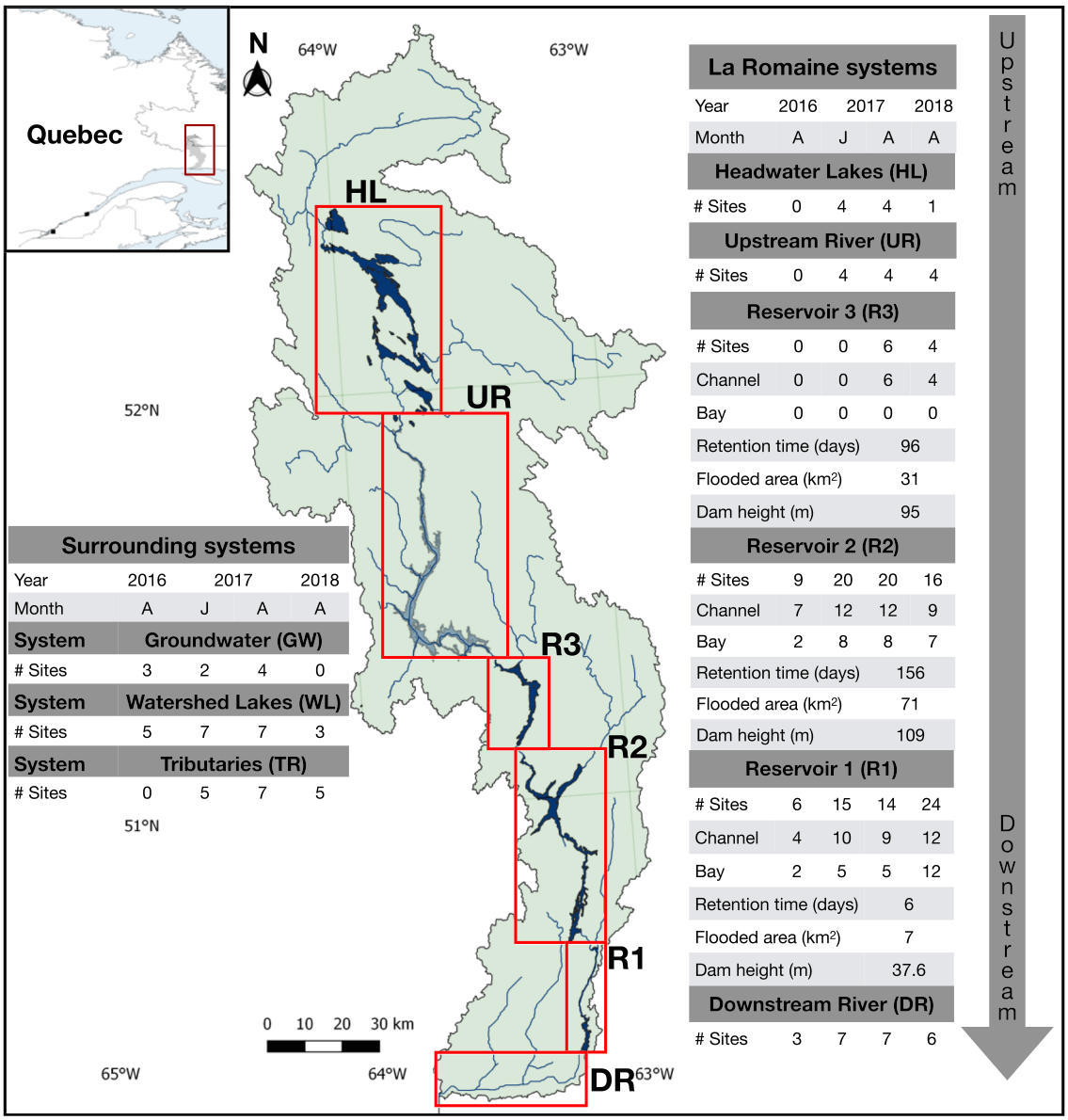


**Figure 1.** Map of the Romaine River watershed in boreal Québec, Canada. In the rectangles are shown the sampled systems from the headwater lakes (HL) to the downstream river (DR). Sampled reservoirs are shown from R1 to R3; the fourth reservoir is represented as the upstream river (UR), since it has yet to be flooded. Groundwater (GW), watershed lakes (WL), and tributaries (TR) are not shown but were sampled in the watershed close to DR, R1, and R2. Tables show the number of sites sampled for all four campaigns as well as the water retention time, flooded area, and dam height for the reservoirs. # Sites refers to the number of sampled sites in a given section of the river (map drawn by F. Rust, 2019).

FDOM, respectively) in acid-washed 125 ml HDPE bottles and 40 ml amber vials respectively using the peristaltic pump. We used a multiparameter probe (YellowSpring Instruments, OH) to measure temperature, pH, and dissolved oxygen (DO), and total depth was obtained with a depth sounder (Hondex). The probe was calibrated daily for pH and DO. Surface water $CO_2$ partial pressure ($pCO_2$ in µatm) and $CH_4$ partial pressure ($pCH_4$ in µatm) were obtained using the headspace equilibrium technique, based on the methods and equation described by Campeau et al. (2014). We used $CO_2$ and $CH_4$ as indirect indicators of carbon processing in oxic and anoxic conditions, respectively (Bastviken et al., 2004; Davies et al., 2003; James et al., 2017). Gas filled aluminum bags were analyzed on the same day they were sampled using an ultraportable GHG analyzer (UGGA, Los Gatos Research).

### 2.3. Chemical Analyses

Preserved water samples were analyzed for aqueous total mercury following the U.S. Environmental Protection Agency (EPA) 1631 protocol with a Tekran 2,600 cold-vapor atomic fluorescence spectrometer (CVAFS) (U.S. Environmental Protection Agency, 2002). Briefly, samples were exposed to bromine monochloride (BrCl) for oxidation and tin chloride ($SnCl_2$) for reduction before volatile Hg(0) collection onto a gold trap following argon-purging. Total mercury concentration was then detected into the CVAFS after a second gold trap amalgamation. Limit of detection (LOD) of the instrument was 0.04 ng $L^{-1}$. New standards (2 ng $L^{-1}$) were analyzed after each 10 sample to assure analytical stability (mean recovery of 103.3 ± 11.5%, $n = 99$). Canadian Association for Laboratory Accreditation (CALA) mercury solutions (C19) were used as an external control solution in each analysis, and the mean (±SD) recovery was 98.5 ± 9.3% ($n = 96$). Analytical field duplicates were processed for each sample with an average relative standard deviation (RSD) of 6.7% with values ranging from 0.75 to 10.7 ng $L^{-1}$.

Analyses for aqueous methylmercury concentrations were based on the 1630 EPA protocol using a Tekran 2700 CVAFS for distilled samples to remove OM and sulfide residues (U.S. Environmental Protection Agency, 2001). Sodium tetraethylborate (NaB $(Et)_4$) was added to help form two volatile mercury species (methyl-ethyl mercury and diethylmercury). The water sample was argon-purged to liberate the volatile species, which were then separated through a gas chromatograph (GC) in the Tekran instrument. Methylmercury was ultimately detected into the cell of the CVAFS. LOD for the Tekran 2700 was 0.01 ng $L^{-1}$. Each 10 samples, standards of 0.5 ng $L^{-1}$ were analyzed and yielded a mean (±SD) recovery of 99.8 ± 9.1% ($n = 154$). We used lobster hepatopancreas reference material (TORT-2) as a reference for MeHg concentrations (mean recovery of 104.4 ± 14.6%, $n = 169$). We ran analytical field duplicates that yielded a RSD of 15.5% for the totality of the samples with values ranging from 0.01 to 0.31 ng $L^{-1}$.

Nutrients were analyzed in duplicates in unfiltered samples for the June and August 2017 campaigns. Total nitrogen (TN) concentrations were measured following the 353.2 EPA method using a flow injection analyzer (Lachat QuikChem 8,000, LOD: 0.7 μg $L^{-1}$). Total phosphorus (TP) concentrations were measured using a segmented flow analyzer (Astoria 2, LOD: 4 μg $L^{-1}$) with the 365.3 EPA method. Certified water (Pérade-09) from Environment Canada was used as a reference material and results were within the acceptance range for reported nutrients. Average concentrations of analytical field duplicates were used for this study.

Metal concentrations in water (including manganese, iron) were quantified by ICP-MS/MS (8900 Agilent) equipped with an SPS 4 autosampler, a quartz spray chamber, and a glass concentric nebulizer with a nickel interface cone, and the He mode was used. LOD for Mn and Fe were of 0.02 and 1.07 μg $L^{-1}$, respectively. Multielement standards (10 μg/$cm^3$, Agilent #8500–6940) were calibrated in a 2.0% $HNO_3$ matrix (grade Omnitrace Ultra, EMD) with the range of 0.0–50 mg/$m^3$ (metals). The laboratory undergoes yearly intercalibration tests for the analyses of Hg and other metal, which respected the criteria of the CALA proficiency testing program.

### 2.4. Dissolved OM Analysis

Water samples for DOC were analyzed using an Aurora 1,030 W TOC Analyzer. Absorbance spectra (190–900 nm) for DOM samples were measured with a Shimadzu UV-1800 spectrophotometer, whereas 3-D fluorescence scans were measured with a Cary Eclipse Fluorescence Spectrophotometer (Agilent Technologies). Emission-excitation matrices were obtained for emission from 240 to 600 by 2 nm increments at excitation 230–450 nm, 5 nm increments using a 1 cm quartz cell. Optical analyses were conducted in the week following the sampling campaign, typically within 2 weeks from collection. Data were corrected for instrument bias, inner filter effect, and Raman scattering prior to parallel factor analysis (PARAFAC) in Matlab using the script from Labrie et al. (https://rdrr.io/github/RichardLaBrie/paRafac_correction/), based on Murphy et al. (2010). Eighty-one additional samples were collected by another team, and fluorescence measurements were performed on a Shimadzu RF5301 PC. We developed a correction matrix to ensure samples from both instruments were comparable.

### 2.5. Statistical Analyses

Statistical analyses and figures were made with R Studio (R Version 3.4.1) using the ggplot2 and factoextra (for the PCA) packages. For sites where all variables were sampled ($n = 96$), we performed a principal

component analyses on centered and scaled data. Differences between the bay and channel sections of the reservoirs were tested using a Welch two sample *t* test for both THg and MeHg concentrations. Data were transformed when necessary to meet normality and homoscedasticity assumptions. The nonparametric Wilcoxon rank sum test was used in cases where data were not normally distributed, such as when we compared the percentage of THg that is MeHg (%MeHg) between natural and flooded systems and between campaigns. Arithmetic means and standard deviation were calculated for most variables among sampling campaign (mean ± SD).

We developed a PARAFAC model in Matlab 8.2 to quantify the different components of the fluorescent DOM in our study sites. This model included samples from this study as well as additional river and lake samples from temperate aquatic ecosystems of Quebec (1,078 samples total) and was developed following the procedure described in Lapierre and Del Giorgio (2014).

## 3. Results

### 3.1. Variability in Environmental Properties Across the Fluvial Network

We found strong spatial and temporal variability in hydrological and environmental conditions across natural and dammed environments that could affect Hg and C cycling. Mean water retention time varied from 6 days in R1 to 156 days in R2 (Table 1), and total depth of the water column at the sampling sites was generally less than 10 m for the upstream river (UR). Watershed lakes and the channel sections in the reservoirs were deeper, especially in the channel of R2 (R2C) where depths could reach over 80 m.

We focused on the analysis of chemical and physical properties for 2017 because for this year we could compare spring and summer conditions and because there was little interannual variation. Oxygen remained close to saturation in nonflooded systems but tended to decrease in reservoir areas, mostly in shallow bays (Table 1). Total nutrient concentrations tended to increase from upstream to downstream, with the highest values found in the bays of R1 (R1B) and some tributaries (TR) for both TP and TN, which ranged from 4.2–26.5 and 32–435 μg $L^{-1}$, respectively. DOC concentrations and pH were relatively stable across the reservoirs and had mean (±SD) values of 5.9 ± 1.3 mg $L^{-1}$(*n = 80)* and 5.6 ± 0.6 (*n = 84)*, respectively. However, tributaries (11.3 ± 6.2 mg $L^{-1}$, *n = 12*) and groundwater (20.0 ± 6.4 mg $L^{-1}$, *n = 5*) sites had higher and more variable DOC concentrations.

There were strong seasonal patterns in terms of the chemical and physical properties of the sampled systems. Water temperature was on average 8°C lower in June (8.2 ± 2.8°C, $n = 68$) than August (16.5 ± 2.3°C, $n = 71$) across all sites, and the ice cover had just melted a few days prior to our June campaign. Reservoirs in June were especially cold, with temperatures occasionally <4°C, as opposed to August during which temperatures were always >14°C. Upstream to downstream trends for nutrients were similar between seasons. For example, TN concentrations increased threefold along the river gradient in June, with values ranging from less than 100 μg $L^{-1}$ in upstream sites to over 300 μg $L^{-1}$ in reservoir bays and sites downstream to the reservoirs. The patterns were similar, with concentrations peaking in reservoir bays for both months, but overall values were higher in June compared to August for both TN and TP. The percentage of DO was lower in the reservoirs, with a marked difference in June when nonflooded sites had an average of 104.5% ($n = 27$) and the average for reservoir sites was 85.3% ($n = 41$). Average values for August were relatively constant around 97% ($n = 67$), but values as low as 82.8% were observed in one bay of R1 reservoir.

### 3.2. Patterns in MeHg Concentrations Along the Reservoir Series and Between Seasons

Overall, lower dissolved MeHg concentrations were found in nonflooded sites compared to reservoir sites. Throughout the years, nonflooded sites upstream of the reservoirs (HL + UR) generally had low concentrations and small ranges of variation in MeHg concentrations (0.05 ± 0.02 ng $L^{-1}$, mean (±SD), $n = 20$; Figure 2a), with only one HL site over 0.08 ng $L^{-1}$. In contrast, we observed consistently higher and more variable values in flooded sites (0.12 ± 0.06 ng $L^{-1}$, $n = 148$) in all 3 years of sampling (Figure 2). Groundwater sites (GW) had low and stable MeHg concentrations in August 2016 (0.045 ± 0.031 ng $L^{-1}$, $n = 3$), June 2017 (0.038 ± 0.004 ng $L^{-1}$, $n = 2$), and August 2017 (0.037 ± 0.036 ng $L^{-1}$, $n = 4$) (Figure 2a).

Concentrations generally increased from upstream to downstream, but they were higher in June than August. Concentrations were over 5 times higher in flooded areas during the spring compared to summer

Water Resources Research

10.1029/2020WR027951

**Table 1**
*Limnological Properties of Surface Waters of Sampled Sites From Three Reservoirs of the Romaine River (R1, R2, and R3) Divided in Channel (C) and Bays (B) and Surrounding Systems From the Watershed (Watershed lakes [WL], Tributaries [TR], Headwater Lakes [HL], and Upstream and Downstream River [UR and DR]) for the June and August 2017 Campaigns*

| | Water temperature (°C) | | Total depth (m) | | pH | | % dissolved oxygen (% DO) |
|---|---|---|---|---|---|---|---|
| System | June | August | June | August | June | August | June |
| WL $n = 7$ | 10.51 ± 3.29 (4.58–13.32) | 18.18 ± 0.66 (17.51–19.51) | 32.6 ± 29.8 (0.8–77.2) | 28.5 ± 21.9 (5.8–64.4) | 5.5 ± 0.3 (5.0–5.9) | 5.2 ± 0.1 (5.0–5.4) | 105.0 ± 4.1 (99.3–109.5) |
| TR $n = 5/7$ | 11.71 ± 0.41 (11.34–12.38) | 14.65 ± 2.02 (11.4–16.9) | 1.5 ± 2.0 (0.3–5) | 1.7 ± 1.5 (0.5–3.9) | 5.6 ± 0.6 (4.9–6.5) | 4.7 ± 0.7 (3.8–5.6) | 107.4 ± 18.7 (91.7–138.2) |
| HL $n = 4$ | 10.55 ± 2.24 (8.16–13.23) | 17.00 ± 0.55 (16.52–17.78) | 7.4 ± 7.5 (1.7–17.9) | 5.3 ± 3.9 (1.2–9.2) | 5.5 ± 0.4 (5.2–6.0) | 5.7 ± 0.4 (5.3–6.4) | 116.0 ± 20.2 (102.5–145.9) |
| UR $n = 4$ | 10.40 ± 1.22 (8.87–11.52) | 16.21 ± 0.53 (15.79–16.98) | 4.7 ± 2.0 (2.6–6.7) | 2.4 ± 0.7 (1.6–3.3) | 5.6 ± 0.2 (5.4–5.8) | 5.7 ± 0.2 (5.5–5.8) | 102.8 ± 1.3 (10.1.5–104.6) |
| R3C $n = 0/6$ | — | 17.58 ± 0.42 (17.15–18.21) | — | 44.6 ± 21.7 (11.6–67.9) | — | 5.7 ± 0.4 (5.3–6.1) | — |
| R2C $n = 12$ | 5.75 ± 1.85 (3.66–9.66) | 18.10 ± 0.71 (16.61–19.3) | 50.6 ± 26.7 (10.8 to >80) | 55.7 ± 19.1 (16.7 to >80) | 5.6 ± 0.4 (4.9–6.1) | 5.4 ± 0.3 (5.0–6.2) | 91.4 ± 12.9 (70.6–110.2) |
| R2B $n = 8$ | 7.80 ± 2.34 (3.88–11.83) | 18.39 ± 0.6 (17.5–19) | 21.7 ± 24.3 (2.1–66.4) | 21.7 ± 20.1 (6.3–61.2) | 5.6 ± 0.4 (4.9–6.1) | 6.1 ± 1.0 (5.4–8.1) | 87.4 ± 8.0 (76.3–102.6) |
| R1C $n = 10/9$ | 6.25 ± 1.27 (4.59–9.16) | 14.38 ± 0.57 (13.7–15.4) | 11.5 ± 9.0 (1.9–30) | 10.7 ± 7.7 (2–25.4) | 5.9 ± 0.5 (5.2–7.0) | 5.3 ± 0.6 (4.6–6.6) | 75.6 ± 17.0 (47.0–97.8) |
| R1B $n = 5$ | 9.80 ± 1.27 (7.57–10.6) | 16.63 ± 1.83 (13.9–19.6) | 6.2 ± 7.4 (1.3–18.6) | 3.3 ± 1.3 (2.1–5.2) | 6.3 ± 0.8 (5.7–7.7) | 5.1 ± 0.4 (4.6–5.4) | 91.6 ± 4.8 (83.9–95.9) |
| DR $n = 7$ | 8.99 ± 1.62 (7–11) | 15.13 ± 0.82 (14.09–16.30) | 3.5 ± 2.0 (0.8–7.1) | 4.2 ± 3.7 (0.7–9.9) | 6.0 ± 0.2 (5.7–6.2) | 5.5 ± 0.2 (5.2–5.7) | 96.3 ± 14.2 (73.2–110.3) |

| | % dissolved oxygen (% DO) | Dissolved organic carbon (DOC) (mg $L^{-1}$) | | Total phosphorus (TP) (μg $L^{-1}$) | | Total nitrogen (TN) (μg $L^{-1}$) | |
|---|---|---|---|---|---|---|---|
| System | August | June | August | June | August | June | August |
| WL $n = 7$ | 95.2 ± 4.1 (87.2–99.6) | 5.22 ± 0.48 (5.94–6.51) | 5.56 ± 0.73 (4.73–6.51) | 6.9 ± 2.7 (4.2–11.8) | 5.8 ± 1.1 (4.3–7.9) | 93.9 ± 50.1 (42.6–185.1) | 148.4 ± 42.9 (118.7–222) |
| TR $n = 5/7$ | 101.2 ± 12.6 (78.6–115.6) | 7.15 ± 2.76 (4.79–11.67) | 13.81 ± 7.01 (4.73–25) | 11.1 ± 1.7 (9.6–13.6) | 10.6 ± 3.3 (6.4–14.3) | 340.7 ± 82.7 (238.2–435.0) | 295.3 ± 85.9 (214.3–415.4) |
| HL $n = 4$ | — | 6.25 ± 0.28 (5.94–6.51) | 5.79 ± 0.38 (5.58–6.35) | 9.4 ± 1.8 (7.6–11.9) | 8.9 ± 0.8 (7.9–9.9) | 59.7 ± 19.8 (46.9–89.1) | 156.6 ± 24.7 (139.0–193.0) |
| UR $n = 4$ | 99.6 ± 1.33 (98.8–101.6) | 6.35 ± 0.12 (6.28–6.52) | 5.92 ± 0.39 (5.62–6.5) | 8.2 ± 0.8 (7.7–9.4) | 8.2 ± 0.8 (7.5–9.3) | 49.6 ± 9.0 (39.7–61.5) | 131.5 ± 9.1 (120.0–140.6) |
| R3C $n = 0/6$ | 96.6 ± 2.9(91.1–99.9) | — | 5.86 ± 0.04 (5.82–5.91) | — | 10.8 ± 1.0 (9.7–12.3) | — | 153.8 ± 8.3 (143.3–166.0) |
| R2C $n = 12$ | 99.8 ± 5.4 (93–113.2) | 5.64 ± 0.81 (3.93–6.86) | 5.73 ± 0.14(5.47–5.93) | 11.6 ± 1.7 (8.9–14.7) | 9.0 ± 2.0 (5.9–12.4) | 146.0 ± 132.1 (32.0–325.9) | 155.0 ± 20.9 (124.4–201.9) |
| R2B $n = 8$ | 98.6 ± 4.0 (91.4–104.3) | 5.68 ± 1.02 (4.73–7.83) | 5.73 ± 0.23 (5.42–6.05) | 11.2 ± 2.9 (8.5–17.3) | 8.3 ± 4.0 (5.2–17.5) | 229.8 ± 125.1 (32.4–376.0) | 187.5 ± 75.7 (136.4–365.2) |
| R1C $n = 10/9$ | 98.3 ± 5.4 (91.2–104.4) | 5.29 ± 0.22 (5.11–5.71) | 6.24 ± 0.34 (5.81–7.02) | 11.9 ± 4.0 (9.5–21.7) | 7.0 ± 0.8 (5.8–8.1) | 289.9 ± 95.5 (83.0–375.4) | 178.3 ± 023.6 (146.8–219.7) |
| R1B $n = 5$ | 81.8 ± 36.2 (8.28–101.5) | 5.2 ± 0.58 (4.86–6.22) | 8.75 ± 3.37 (5.5–14.14) | 12.6 ± 2.7 (8.9–15.7) | 13.5 ± 7.6 (7.7–26.5) | 326.6 ± 127.2 (102.4–404.5) | 274.7 ± 91.5 (179.1–391.5) |
| DR $n = 7$ | 99.6 ± 8.2 (9.18–113.4) | 5.18 ± 0.19 (4.93–5.52) | 6.25 ± 0.68 (5.77–7.71) | 11.3 ± 1.3 (10.1–13.8) | 9.8 ± 2 (7.0–13.4) | 218.5 ± 139.3 (65.3–369.7) | 171.1 ± 33.0 (131.0–222.9) |

*Note*. Shown in the cells are the means of each variable for the sampled sites of each system with the standard deviation. In brackets are the minimum and maximum values. Systems where the number of sites ($n$) are not separated by a slash bar means that the same number of sites were sampled in June and in August. R3 was not sampled in June for safety purposes as the reservoir was being flooded and floating trees were blocking the way. Headwater lakes could not be sampled for DO in August due to logistic reasons.

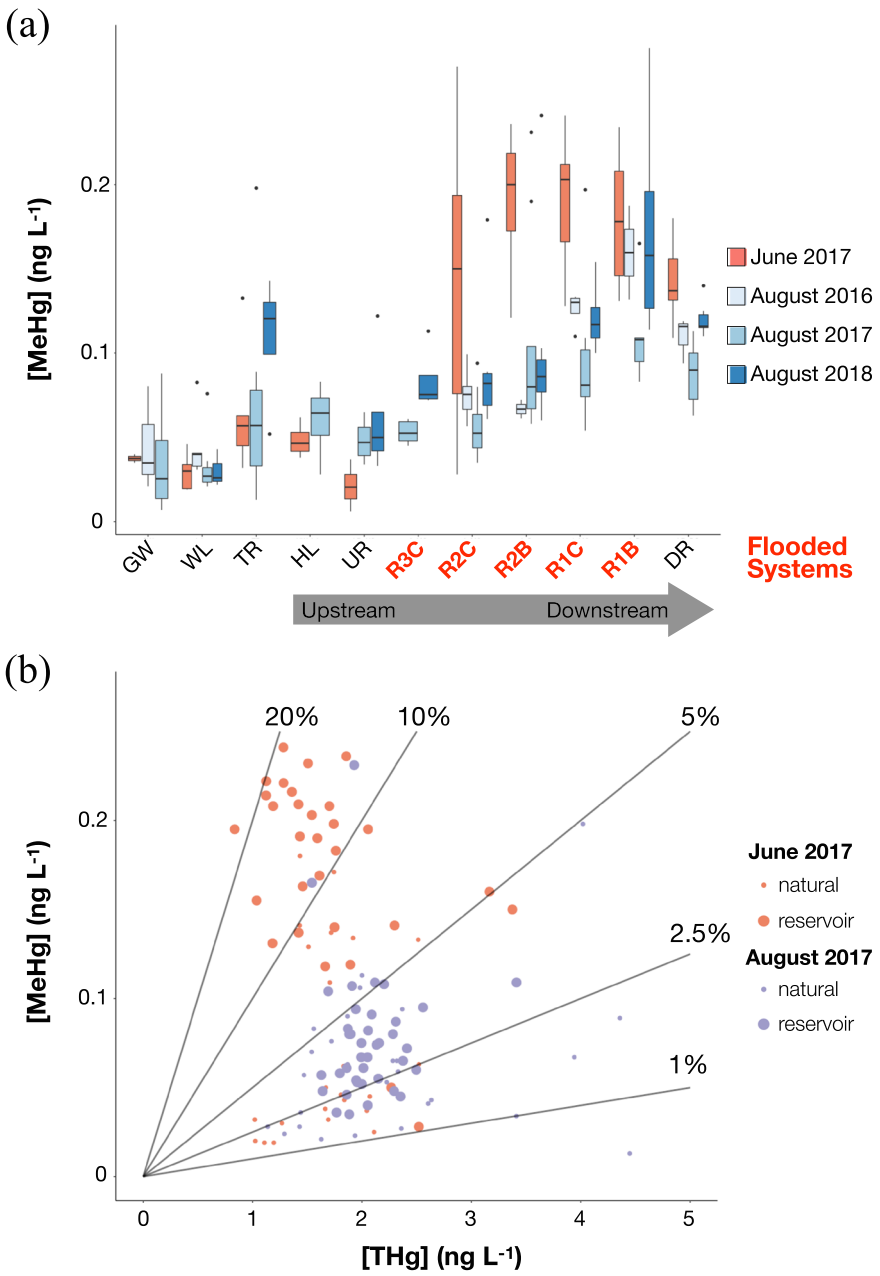


**Figure 2.** (a) Boxplot representing dissolved methylmercury concentrations in ng L-1 across the nonflooded and flooded sites in the catchment of the Romaine River for the 2016, 2017, and 2018 campaigns where hinges represent the 25th, 50th, and 75th percentiles starting from the bottom, whisker length is determined by 1.5 * interquartile range (dots are considered outliers). Site categories are broadly positioned on an upstream-downstream gradient. (b) Regression of the concentrations of MeHg as a function of THg for the two 2017 campaigns. Lines represent the % of THg as MeHg. Groundwater sites were not included in the correlation plot due to high THg values (average THg = 7.67 ng $L^{-1}$ for the two campaigns) and low MeHg values (0.037 ng $L^{-1}$ for the two campaigns), likely due to the presence of particles, which highly skewed the pattern. One tributary site sampled in August presenting an extreme value was also excluded (MeHg = 0.023 ng $L^{-1}$, THg = 9.71 ng $L^{-1}$). Abbreviations and number of sampled sites are detailed in Figure 1.

2017 (Figure 2). There was a peak of mean concentrations in June (0.191 ± 0.041 ng $L^{-1}$, $n = 8$) in the bays of the R2 reservoir (R2B) and concentrations were at their highest in the most downstream reservoir (R1) for all August campaigns.

#### 3.2.1. Contrasting Spatial and Temporal Patterns for THg Versus MeHg

There were no systematic patterns in THg concentrations when comparing nonflooded versus reservoir sites, or on an upstream-downstream gradient in the reservoir sequence (Figures 2b and S1 in the supporting information). Furthermore, Figure 2b shows a relatively narrow range for [THg], as opposed to [MeHg], which varied up to tenfold across systems. Combined with the strong downstream increasing pattern for [MeHg], the lack of spatial pattern for [THg] resulted in no relationship between these two forms of mercury within the network (Figure 2b), suggesting a decoupling in the loading or transformation of these two forms of Hg. Similar patterns were found for unfiltered MeHg and THg through the system and the seasons. For instance, in 2017, simple linear regression models were calculated for both variables to explore the correlation between unfiltered and filtered samples. In both cases, filtered samples where correlated with unfiltered samples for MeHg ($R^2$ adj = 0.77, $p < 0.0001$, $n = 127$) and THg ($R^2$ adj = 0.84, $p < 0.0001$, $n = 122$) and followed the following equations including the standard errors for the slope and the intercept (SE):

$$[MeHg]_{filtered} = 0.66 \pm 0.03\ [MeHg]_{unfiltered} + 0.030 \pm 0.004 \quad (1a)$$

$$[THg]_{filtered} = 0.83 \pm 0.03\ [THg]_{unfiltered} - 0.01 \pm 0.09 \quad (1b)$$

Since several of our predictive variables were analyzed in filtered samples, we focused on the dissolved Hg samples in the results section.

There were no clear intrareservoir patterns for THg or MeHg. Sites in bays appeared to have higher concentrations of MeHg (but not THg; Figures 2a and S1) in R1 and R2 reservoirs, compared to channel sites, but there were no statistically different concentrations of THg and MeHg between bay and channel sites of reservoirs when all sites were analyzed together. On the other hand, there were major differences in the seasonal patterns of total versus methylated Hg. In particular, [THg] had the same range between seasons, but [MeHg] was systematically higher in June compared to August in 2017 (Figure 2a). For flooded sites in June, [MeHg] represented between 10% and 20% of THg (11.6 ± 5.1%, $n = 34$) but nonflooded sites had significantly lower values (4.4 ± 3.3%, $n = 23$) (Wilcoxon test: $p < 0.001$). Mean %MeHg for the month of August in reservoir (4.2 ± 2.3%) and nonflooded sites (2.9 ± 1.5%) were also significantly different (Wilcoxon test: $p = 0.012$), but values varied less. Reservoir sites showed higher %MeHg in June (Wilcoxon test: $p < 0.001$), but nonflooded sites had similar concentrations in both seasons (Wilcoxon test: $p = 0.22$). Overall, we found strong patterns in MeHg concentrations along the river to reservoir continuum and between seasons that were largely decoupled from THg concentrations, which suggests that a significantly higher proportion of the ambient THg was methylated in spring compared to summer (Figure 2b).

### 3.3. Hydrological and Biogeochemical Controls on MeHg Concentrations

Contrary to our hypothesis, MeHg was inversely related to temperature, a trend that was generated mostly by the higher concentrations and proportions of MeHg occurring during the June sampling (Figure 2). This pattern is apparent in a principal component analysis that shows the overall relationships between mercury and dissolved organic carbon pools with environmental drivers (Figure 3). In particular, MeHg and %MeHg from June and August were strongly, negatively associated with Axis 1, opposite to temperature. The distribution of the sites along the second axis was driven by environmental variables, such as TP, $pCH_4$ (positive scores on Axis 2), and pH and %DO (negative scores on Axis 2; Figure 3).

Concentrations of THg were, as expected, related to concentrations of DOC and colored DOC (CDOM), the latter representative of terrestrial sources. However, contrary to our expectations, there was no relationship between concentrations or proportions of MeHg with either the concentrations or composition of DOC, as determined by its optical properties. We quantified patterns in DOC composition using PARAFAC modeling of fluorescence scans, which identified five components (Figure S2) corresponding to commonly identified humic or fulvic material with a dominant terrestrial origin (C1, C2, and C4) and to microbial-derived or protein-like material associated to recent production on land or in the water (C3 and C5) (Lapierre & del Giorgio, 2014; Wünsch et al., 2019). We found that THg covaried more strongly with humic-like C2 and C4, as well as with bulk DOC. On the other hand, MeHg was only weakly correlated to DOC and not related at all to protein-like C3 and C5. The strongest association for MeHg concentration and proportion was with

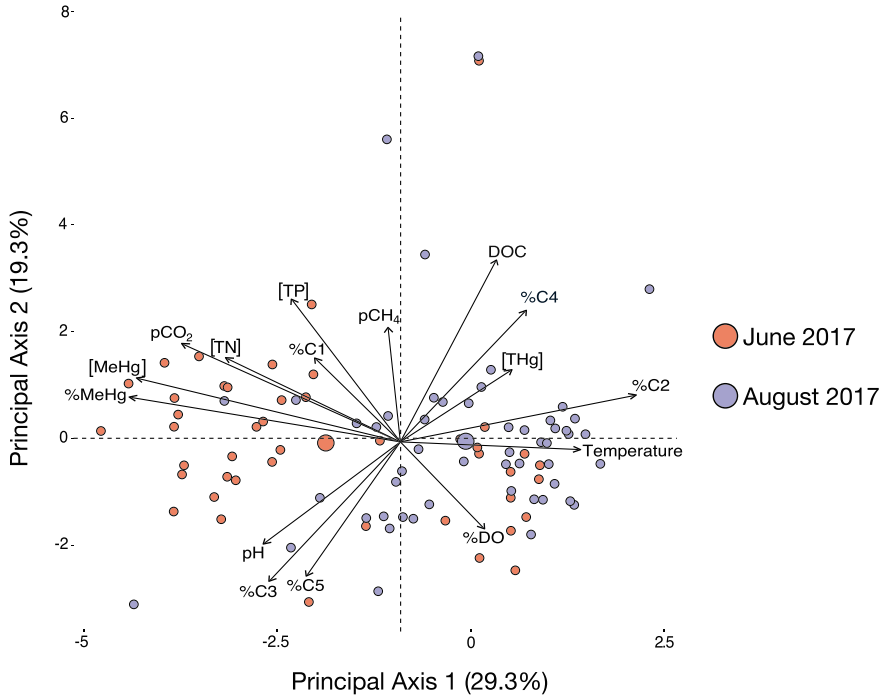


**Figure 3.** Principal component analysis (PCA) representing mercury (THg, MeHg, and %MeHg) and carbon (DOC and %C1 to %C5 representing the relative proportion of each PARAFAC component) groups in relation to environmental conditions for the 2017 field campaigns. Larger points denote the centroid of all sites for each campaign. Sample size for June is 44 and 52 for August. Forty-four sites (mostly upstream sites sampled from the floatplane) were excluded from the PCA as not all variables were systematically collected at each station.

$pCO_2$ (Figure 3), suggesting that there is indeed a coupling between the processing of Hg and C in the studied systems but that this coupling was most apparent with the gases rather than with the relative abundance of specific DOC pools.

### 3.4. Covariation of MeHg and $pCO_2$ Across the Reservoir Complex

The spatial patterns for $pCO_2$ mirrored the spatial patterns for MeHg, sharply increasing entering the reservoir (Figure 4a). In June, $pCO_2$ in nonflooded upstream sites and watershed lakes consistently remained <1,000 μatm (901.08 ± 147.11 μatm, $n = 15$), but $pCO_2$ in R2C and R2B increased over 2,000 μatm. A similar pattern was observed in August, but values were lower, and the peak concentrations were found further downstream in R1 (Figure 4a), similar to what has been observed for MeHg (Figure 2a). MeHg and $pCO_2$ were strongly correlated across the natural and flooded systems ($R^2$ adj = 0.57, $p < 0.0001$), and this correlation holds for both seasons (Figure 4b). The relationship followed the following equation with SE for the slope and intercept:

$$[MeHg] = 7.67e^{-5} \pm 6.11e^{-6} pCO_2 - 1.20e^{-2} \pm 0.51e^{-3} \quad (2)$$

## 4. Discussion

### 4.1. The Role of a Boreal Reservoir Complex in the Transformation Versus Mobilization of Mercury

Contrary to our expectations, we found no observable pattern in THg distribution along a fluvial network continuum that included nonflooded as well as flooded sites distributed along three consecutive reservoirs. This was especially surprising since all of them were all sampled less than 4 years since commissioning. Previous studies of boreal reservoirs in similar climatic settings have shown that THg was 1.5 times higher compared with preimpoundment concentrations in the weeks following impoundment (Lucotte et al., 1999).

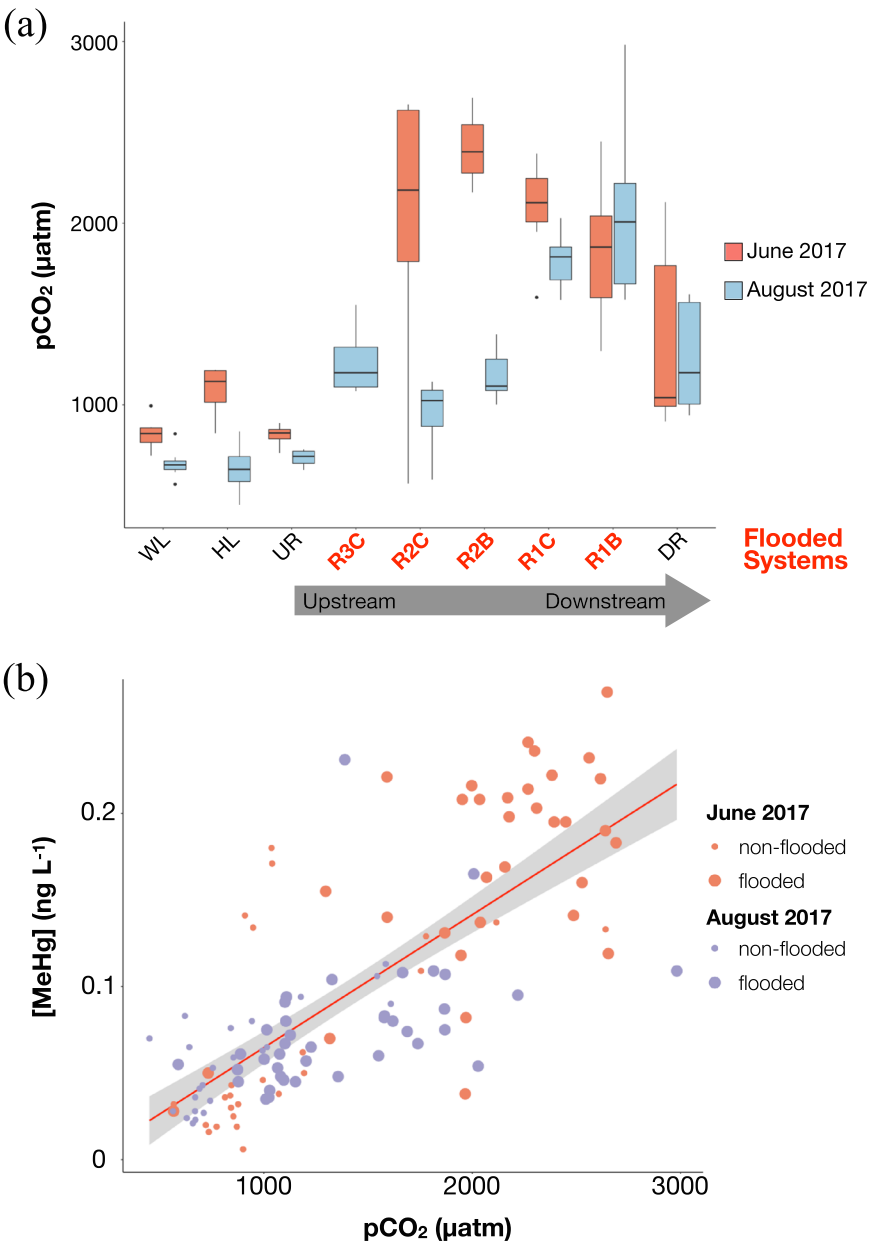


**Figure 4.** (a) Surface water $pCO_2$ (µatm) through the aquatic continuum of the Romaine River. Abbreviations and sample size for each site are detailed in Figure 1. (b) Regression between MeHg concentrations and $pCO_2$ for June and August 2017 in natural ($n$ = 47 [June = 24, August = 23]) and flooded ($n$ = 72 [June = 33, August = 39]) sites.

THg rose by a factor of 3 in the 6 months following flooding (Li et al., 2013) in a subtropical reservoir of the Wujiang River. It is possible that we missed the peak Hg increase in the R1 and R2 reservoirs, which were already 2 and 3 years old when we first sampled them. However, in 2017, we sampled the R3 reservoir only a few months following flooding, and we did not observe higher concentrations of THg. This was the case although there were considerable amounts of vegetation flooded, to a point where sampling was not possible in the downstream portions of R3 in 2017, close to the dam, because thousands of floating trees were blocking the way. Considering the steep catchment slopes surrounding the river, the relatively thin soils and the low abundance of wetlands within the watershed, THg inputs due to flooding may be reduced (Mailman et al., 2006) compared to other systems in comparable latitudes. A key factor may be the low ratio of area of land flooded relative to the volume of these reservoirs, which due to the local

topography is much lower than for most reservoirs in boreal Québec, which tend to much larger but shallower. This either suggests that if there were initial peaks in THg following impoundment, concentrations in the Romaine reservoirs rapidly decreased to baseline levels, or more likely (given the lack of increase in R3 following impoundment), that damming did not lead to observable increases in dissolved THg in these deep, canyon-shaped reservoirs with relatively small flooding areas.

Concentrations of MeHg, on the other hand, consistently increased from nonflooded to reservoir sites, and from upstream to downstream along the reservoirs sequence. In particular, there was a significant, about twofold increase along the reservoir sequence in August, and an about fivefold increase in June. This trend agrees with previous studies reporting systematic increases in MeHg concentrations upon flooding in inundated areas (Brigham et al., 2002; Coquer et al., 2003; Kelly et al., 1997; St. Louis et al., 2004; Zhao et al., 2017) and increases from upstream to downstream in a dammed river (Zhao et al., 2017). For example, Kasper et al. (2014) observed concentrations of 0.11 – 0.18 ng $L^{-1}$, 0.5 km downstream from the reservoir, comparable to our range of measures from the river stretch, which collects water from the bottom waters of R1 (0.06 – 0.18 ng $L^{-1}$). These trends of elevated MeHg in reservoirs have been explained by the fact that flooding leads to the formation of anoxic environments within the newly created aquatic environments, where Hg methylation can proceed (Kasper et al., 2014). Degradation of freshly flooded OM has been shown to promote anoxia in sediments and bottom waters of newly created reservoirs, which in turn favors Hg methylation (Hall et al., 2005; Roy et al., 2009). Hypoxia or occasional anoxia at the sediment-water interface can also enhance transport of mercury from the sediments to the water column (Feyte et al., 2012). Such redox gradients also affect the release of Mn and Fe from sediments (Pakhomova et al., 2007). In our study, Fe and Mn surface concentrations were correlated with each other and with $CO_2$ partial pressure ($pCO_2$) and MeHg, both presenting higher values in June compared to August 2017 (Figure S3). Together these variables suggest that there was high OM processing by microbes, resulting in signs of anoxia that may have developed locally or seasonally in our studied systems. Therefore, our results suggest that favorable conditions for Hg methylation were more prominent in reservoir versus nonflooded sites and that MeHg production exceeded losses in reservoirs.

Despite the significant increases compared to nonflooded systems, concentrations of MeHg measured in the reservoirs of the Romaine remained at the lower end of concentrations reported in reservoirs within comparable geographic contexts. For example, concentrations averaging 0.28 $\pm$ 0.10 ng $L^{-1}$ have been observed in La Grande complex in boreal Quebec in the 3 years following a flooding event (Montgomery et al., 2000), and around 0.19 ng $L^{-1}$, during flooding of the Muskrat Falls reservoir in Newfoundland (Calder et al., 2016). High concentrations were found in the discharged water of a temperate reservoir in New Mexico, peaking at 1.14 ng $L^{-1}$ in the summer, but surface water concentrations were generally lower and only reached 0.26 ng $L^{-1}$ after the fall turnover (Canavan et al., 2000). In a tropical setting, MeHg concentrations were several fold higher (0.5 – 0.6 ng $L^{-1}$) than those found in the Romaine, due to high THg concentrations combined with high proportion of MeHg ranging from 20 – 35% (Coquer et al., 2003). Overall, we observed a gradual accumulation of MeHg once entering the reservoir sequence compared to nonflooded systems in the catchment, which presumably originated from anoxic zones in deep parts of the highly dynamic main channel and shallower hypolimnia of the flooded bays, which may be more prominent than in nonflooded sites. However, given the steep catchment and boreal climate, MeHg concentrations remained in the lower end of the range observed in other boreal and nonboreal reservoirs.

The increase in MeHg along the reservoir sequence combined with the lack of spatial patterns for THg suggests a decoupling of the processes leading to the mobilization *versus* transformation of mercury in our study system. While previous studies have found consistent positive correlations between MeHg and THg in nonflooded (Kelly et al., 1995; MacMillan et al., 2015) and flooded systems (Bravo et al., 2010; Montgomery et al., 2000; Roy et al., 2009), we found no significant relationship between both pools of THg and its methylated form. Hence, in the Romaine reservoirs, high MeHg concentrations are due to a higher proportion of methylated mercury for a similar THg pool (Figure 2). A comparable increase in %MeHg has been observed in dammed versus nondammed systems in other regions. For example, %MeHg in Quebec boreal reservoirs was higher on average (12%) than in surrounding lakes and rivers (3%, Montgomery et al., 2000), and similar trends were observed in a tropical reservoir where the %MeHg in the bottom waters was around 20% compared to 1.0 – 1.7% in surrounding rivers and of 1.8% in surface waters (Coquer et al., 2003). The

contrasting spatial patterns for MeHg versus THg may further be explained by the fact that, in addition to promoting Hg methylation, reservoirs may contribute to enhanced THg sedimentation as it is mostly bound to particles, which settle close to dams, counterbalancing potential increase in THg remobilization. For example, in a recent study, THg levels diminished along a series of cascade reservoirs, whereas MeHg increased with every consecutive reservoir (Zhao et al., 2017). Therefore, the fact that THg was less variable in the Romaine reservoir continuum could be due to an equilibrium between sedimentation, inputs and its transformations, as seen by the increase in %MeHg in the reservoirs. Nonflooded upstream and surrounding sites (groundwater, tributaries, and lakes), on the other hand, generally had low and stable MeHg concentrations throughout the years compared to flooded sites; hence, they did not seem to act as an external source of methylmercury for the reservoir. Therefore, it appears that sources of MeHg exceeded sinks along the reservoirs sequence, leading to a gradual accumulation flowing from upstream to downstream.

### 4.2. Linking Functional Pools of Carbon and Mercury Across a Boreal Reservoir Complex

Recent studies have found strong relationships between total DOM concentrations, and in particular, terrestrial DOM pools with THg concentrations (Bravo, Kothawala, et al., 2018; Lavoie et al., 2019), because Hg is bound to DOM and they are comobilized from land to water. Interestingly, when all sites were considered (including tributaries and groundwater that had higher values), we observed a slope of 0.28 ng/mg in the linear regression between THg and DOC, comparable to the average global slope identified in a recent meta-analysis for freshwater (Lavoie et al., 2019). We also observed an association between concentrations of DOC, DOM components C2 and C4 (identified in our PARAFAC model as humic-like DOM presumably of terrestrial origin) and THg, suggesting that colored, terrestrial DOC is a good proxy for the loading of Hg in the Romaine watershed.

As opposed to THg, concentrations of MeHg showed unexpectedly weak relationships with environmental and DOM properties, as well as counterintuitive seasonal patterns, being significantly higher in the colder June month of 2017 along the reservoir sequence. First, this is surprising since warmer temperature typically enhance the conditions that favor methylation (i.e., anoxia; Ullrich et al., 2001; Paranjape & Hall, 2017) and export of MeHg by hydroelectric reservoirs in other regions typically peak during summer (Canavan et al., 2000; Zhao et al., 2017). Moreover, we expected DOM pools associated to recent production (e.g., protein-like C3 and C5; see Lapierre & Del Giorgio, 2014) to be related to concentrations of MeHg, as has been shown in recent studies (Bravo et al., 2017; Bravo, Kothawala, et al., 2018; Herrero Ortega et al., 2018), because high abundance or proportion of these DOM pools are often found in warm, productive sites and would represent high biological activity in the water column or in the sediments that may co-occur with Hg methylation. However, no DOM quantity or quality (i.e., PARAFAC components) variable was related to MeHg concentrations or proportions. Excluding the tributary and groundwater sites, the range of variation for DOC concentrations throughout the reservoirs and surrounding systems (WL, HL, UR, and DR) was relatively small for both months ($5.84 \pm 1.11$ mg $L^{-1}$, $n = 123$). Three bay sites only, in August, presented values over 10 mg $L^{-1}$ (10.05 – 14.14 mg $L^{-1}$), while other sites were always below 7.9 mg $L^{-1}$. Nonetheless, this is a narrow range compared to other studies that found a link between locally produced DOM and MeHg. For example, Bravo, Kothawala, et al. (2018) observed DOC concentrations ranging from 0.9 – 18.5 mg $L^{-1}$ in streams, and Bravo et al. (2017) observed DOC concentrations ranging from 3.8 – 33.1 mg $L^{-1}$ in boreal lakes. Results from Lescord et al. (2018) also showed higher mean DOC concentrations in boreal (~10 mg $L^{-1}$) lakes and streams (~22.2 mg $L^{-1}$) with a large range for both lakes (5.4 – 16.2) and streams (14.4 – 29.1 mg $L^{-1}$). They also found lower MeHg concentrations ($0.038 \pm 0.016$ ng $L^{-1}$ in streams and $0.017 \pm 0.013$ $L^{-1}$ in lakes) than in the natural systems sampled in our study, suggesting that higher DOC does not systematically lead to higher concentrations and proportions of MeHg. Therefore, as opposed to recent studies, we could not find a link between DOC composition and Hg speciation within the narrow DOC range observed in natural and dammed systems of the Romaine River watershed.

Our findings suggest that factors other than local environmental drivers of Hg methylation, such as high temperature or low pH, explain MeHg concentration at any given site; hence, that much of the measured MeHg across the reservoir sequence has been produced elsewhere. Although we did find high concentrations suggestive of local production in warm and shallow bays in August (Figure 2a), the overall seasonal pattern led to much stronger temporal patterns compared to intrareservoir patterns. We found that the strongest predictor of MeHg concentrations and %MeHg was the partial pressure of $CO_2$ ($pCO_2$) rather

than DOM concentrations or composition, temperature or any other environmental variable typically associated to MeHg dynamics (Figures 3 and 4). MeHg and $pCO_2$ followed the same spatial pattern for the spring and summer campaigns of 2017, where increases of MeHg concentrations were concurrent with spikes of $CO_2$ in the reservoirs. As for MeHg, $pCO_2$ showed strong upstream-downstream as well as seasonal patterns, suggesting that it reflects a cumulative carbon processing through the reservoir and that this carbon processing may have led to environmental conditions favorable for Hg methylation.

### 4.3. The Importance of Connectivity and Winter Processes

The flooding of large areas is known to create conditions that are prone for both GHG production and Hg methylation. Links between MeHg and GHG have previously been found in an experimental flooded area, as well as in small ponds and lakes in northern Canada (Kelly et al., 1997; MacMillan et al., 2015). Kelly et al. (1997) found that flooded vegetation in peatlands stimulated microbial production of $CO_2$ and $CH_4$ and that methylation of inorganic mercury increased. However we have not found any correlation between $CH_4$ and MeHg in surface waters, unlike other studies (MacMillan et al., 2015), possibly due to $CH_4$ being oxidized in $CO_2$ during its transport from the deep parts of the water column to surface waters (Barros et al., 2011; Bastviken et al., 2004). Therefore, in highly connected systems with high water retention time such as the Romaine River it appears that accumulation through the reservoir sequence is more important than immediate, local production in explaining MeHg and GHG patterns at the whole-system level.

The spatial and seasonal patterns we measured for MeHg in 2017 suggest a net accumulation during the winter that is flushed through the reservoir sequence with ice-off. The spring sampling was conducted in early June, which, in this region, corresponded to barely 2 weeks following ice-off. Under ice cover, the water column becomes shallower and isolated from the atmosphere, and potentially more stratified; any of these factors would favor anoxia in portions of the water column and close to sediments, hence to a production of MeHg. It is unlikely that methylation rate in any given anoxic environment is higher in the winter, because of lower temperatures, but it is possible that a greater proportion of the water column and sediments in the reservoirs and their upstream lakes become anoxic during the winter, such that methylation rates surpass demethylation during this time of the year. In another study on boreal reservoirs, one of the highest MeHg measurements was taken under the ice, in a flooded shallow area where the water became stagnant leading to depleted DO concentrations (Montgomery et al., 2000). A recent study conducted on the Three Gorges Reservoir also found strong seasonal patterns in MeHg concentrations with values higher in winter and spring due to an increase in water level and an effect of accumulation in the reservoir (Liu et al., 2019). In the Romaine reservoirs, lower oxygen concentrations that have been observed in June versus August 2017 (Table 1), concurring with higher $CO_2$ concentrations in June (Figure 4b). While the oxygen levels in the reservoirs in June were far from being anoxic, lower concentrations may reflect the mixing of deep anoxic waters with surface waters that would otherwise be rich in oxygen, as suggested by oversaturated oxygen levels in the surrounding natural systems (Table 1). This seems to be supported by higher concentrations of Mn and Fe in June, as well as their correlation with MeHg and $pCO_2$ (Figure S3), as their release from sediments are favored in low oxygen conditions (Pakhomova et al., 2007).

Given the water retention time of over 150 days in R2 (Table 1), it is likely that a proportion of the measured MeHg in R1 in August (about 70 days later) was produced during the last winter, as water turnover upon ice-melt can mobilize MeHg produced at the sediment-water interface to the surface waters (Long et al., 2014). However, upstream MeHg is probably not the only source in R1 because while $pCO_2$ is higher in bays in August (Figure 4), it is more likely that these high $pCO_2$ are sustained by biological processing in the bays because the high gas exchange coefficients in these large systems would have evaded the $CO_2$ coming from R2 along the way (Rust et al., in preparation). Together, these results suggest that there were reducing conditions under ice (in the sediments and possibly the overlying water) and in shallow and productive bays that led to the release of MeHg from sediments and its accumulation in the water during the winter, which led to a MeHg accumulation from upstream to downstream and to the high MeHg concentrations observed at ice-off in June compared to August.

Better understanding the processes behind the patterns of MeHg in these engineered systems, and in particular, the timing in peak concentrations may help refine whole-system budgets as well as guide management, for example, to better predict the environmental impacts of water drawdown at different times of

the year. We suggest that further studies on mercury methylation under the ice and during ice melt should be conducted as these factors could help refine annual Hg budgets in systems with long residence times.

## Data Availability Statement

Data used in the analyses and figures is publicly available online (at http://doi.org/10.5281/zenodo.4004838).

**Acknowledgments**
We are grateful to Dominic Bélanger, Caroline Fink-Mercier, Justine Lacombe-Bergeron, François Fournel, and Serge Paquet as well as the Lapierre, Amyot, and del Giorgio laboratory members for their help with field sampling, logistics, and laboratory analysis. Fieldwork organization at the Romaine would not have been possible without help from the Carbon Biogeochemistry of Boreal Aquatic Systems (CarBBAS) research chair team and our guide, Pierre Desjardins, from Uanan Experts-Conseils Inc. We are thankful to Sandra Ann Binning and Jan Franssen for commenting on a preliminary version. Funding for this study was provided by Hydro-Québec, NSERC, the Canada Research Chair Program, and the ÉcoLac FONCER-CRSNG scholarship program.

## References

Amos, H. M., Jacob, D. J., Kocman, D., Horowitz, H. M., Zhang, Y., Dutkiewicz, S., et al. (2014). Global biogeochemical implications of mercury discharges from rivers and sediment burial. *Environmental Science and Technology*, *48*(16), 9514–9522. https://doi.org/10.1021/es502134t

Anderson, M. R. (2011). Duration and extent of elevated mercury levels in downstream fish following reservoir creation. *River Systems*, *19*(3), 167–176. https://doi.org/10.1127/1868-5749/2011/019-0023

Barros, N., Cole, J. J., Tranvik, L. J., Prairie, Y. T., Bastviken, D., Huszar, V. L. M., et al. (2011). Carbon emission from hydroelectric reservoirs linked to reservoir age and latitude. *Nature Geoscience*, *4*(9), 593–596. https://doi.org/10.1038/ngeo1211

Bastviken, D., Cole, J., Pace, M., & Tranvik, L. (2004). Methane emissions from lakes: Dependence of lake characteristics, two regional assessments, and a global estimate. *Global Biogeochemical Cycles*, *18*, GB4009. https://doi.org/10.1029/2004GB002238

Beutel, M., Fuhrmann, B., Herbon, G., Chow, A., Brower, S., & Pasek, J. (2020). Cycling of methylmercury and other redox-sensitive compounds in the profundal zone of a hypereutrophic water supply reservoir. *Hydrobiologia*, *3*, 1–22. https://doi.org/10.1007/s10750-020-04192-3

Bravo, A. G., Bouchet, S., Tolu, J., Björn, E., Mateos-Rivera, A., & Bertilsson, S. (2017). Molecular composition of organic matter controls methylmercury formation in lakes. *Nature Communications*, *8*(1), 1–9. https://doi.org/10.1038/ncomms14255

Bravo, A. G., Kothawala, D. N., Attermeyer, K., Tessier, E., Bodmer, P., Ledesma, J. L. J., et al. (2018). The interplay between total mercury, methylmercury and dissolved organic matter in fluvial systems: A latitudinal study across Europe. *Water Research*, *144*, 172–182. https://doi.org/10.1016/j.watres.2018.06.064

Bravo, A. G., Loizeau, J., & Dominik, J. (2010). Reservoirs as a trap for pollutants: Mercury in the Babeni Reservoir. *NEAR Curriculum in Natural Environmental Sciences*, *88*, 211–219.

Bravo, A. G., Peura, S., Buck, M., Ahmed, O., Mateos-Rivera, A., Ortega, S. H., et al. (2018). Methanogens and iron-reducing bacteria: The overlooked members of mercury-methylating microbial communities in boreal lakes. *Applied and Environmental Microbiology*, *84*(23). https://doi.org/10.1128/AEM.01774-18

Brigham, M. E., Krabbenhoft, D. P., Olson, M. L., & DeWild, J. F. (2002). Methylmercury in flood-control impoundments and natural waters of northwestern Minnesota, 1997–99. *Water, Air, and Soil Pollution*, *138*(1/4), 61–78. https://doi.org/10.1023/A:1015573621474

Calder, R. S. D., Schartup, A. T., Li, M., Valberg, A. P., Balcom, P. H., & Sunderland, E. M. (2016). Future impacts of hydroelectric power development on methylmercury exposures of Canadian indigenous communities. *Environmental Science and Technology*, *50*(23), 13,115–13,122. https://doi.org/10.1021/acs.est.6b04447

Campeau, A., Lapierre, J., Vachon, D., & Del Giorgio, P. A. (2014). Global biogeochemical cycles boreal landscape of Québec. *Global Biogeochemical Cycles*, *28*, 57–69. https://doi.org/10.1002/2013GB004685.Received

Canavan, C. M., Caldwell, C. A., & Bloom, N. S. (2000). Discharge of methylmercury-enriched hypolimnetic water from a stratified reservoir. *Science of the Total Environment*, *260*(1–3), 159–170. https://doi.org/10.1016/S0048-9697(00)00560-X

Celo, V., Lean, D. R. S., & Scott, S. L. (2006). Abiotic methylation of mercury in the aquatic environment. *Science of the Total Environment*, *368*(1), 126–137. https://doi.org/10.1016/j.scitotenv.2005.09.043

Chadwick, S. P., Babiarz, C. L., Hurley, J. P., & Armstrong, D. E. (2006). Influences of iron, manganese, and dissolved organic carbon on the hypolimnetic cycling of amended mercury. *Science of the Total Environment*, *368*(1), 177–188. https://doi.org/10.1016/j.scitotenv.2005.09.039

Compeau, G. C., & Bartha, R. (1985). Sulfate-reducing bacteria: Principal methylators of mercury in anoxic estuarine sediment. *Applied and Environmental Microbiology*, *50*(2), 498–502. https://doi.org/10.1128/AEM.50.2.498-502.1985

Coquer, M., Cossa, D., Azemard, S., Peretyazhko, T., & Charlet, L. (2003). Methylmercury formation in the anoxic waters of the Petit-Saut reservoir (French Guiana) and its spreading in the adjacent Sinnamary River. *Journal de Physique IV (Proceedings)*, *107*, 327–331. https://doi.org/10.1051/jp4:20030308

Dalzell, B. J., Filley, T. R., & Harbor, J. M. (2005). Flood pulse influences on terrestrial organic matter export from an agricultural watershed. *Journal of Geophysical Research: Biogeosciences*, *110*, G02011. https://doi.org/10.1029/2005JG000043

Davies, J. M., Hesslein, R. H., Kelly, C. A., & Hecky, R. E. (2003). $PCO_2$ method for measuring photosynthesis and respiration in freshwater lakes. *Journal of Plankton Research*, *25*(4), 385–395. https://doi.org/10.1093/plankt/25.4.385

Denfeld, B. A., Baulch, H. M., del Giorgio, P. A., Hampton, S. E., & Karlsson, J. (2018). A synthesis of carbon dioxide and methane dynamics during the ice-covered period of northern lakes. *Limnology and Oceanography Letters*, *3*(3), 117–131. https://doi.org/10.1002/lol2.10079

Ducharme-Riel, V., Vachon, D., del Giorgio, P. A., & Prairie, Y. T. (2015). The relative contribution of winter under-ice and summer hypolimnetic $CO_2$ accumulation to the annual $CO_2$ emissions from northern lakes. *Ecosystems*, *18*(4), 547–559. https://doi.org/10.1007/s10021-015-9846-0

Feyte, S., Gobeil, C., Tessier, A., & Cossa, D. (2012). Mercury dynamics in lake sediments. *Geochimica et Cosmochimica Acta*, *82*, 92–112. https://doi.org/10.1016/j.gca.2011.02.007

Fleming, E. J., Mack, E. E., Green, P. G., & Nelson, D. C. (2006). Mercury methylation from unexpected sources: Molybdate-inhibited freshwater sediments and an iron-reducing bacterium. *Applied and Environmental Microbiology*, *72*(1), 457–464. https://doi.org/10.1128/AEM.72.1.457-464.2006

Friedl, G., & Wüest, A. (2002). Disrupting biogeochemical cycles—Consequences of damming. *Aquatic Sciences*, *64*(1), 55–65. https://doi.org/10.1007/s00027-002-8054-0

Gilmour, C. C., & Henry, E. A. (1991). Mercury methylation in aquatic systems affected by acid deposition. *Environmental Pollution*, *71*(2–4), 131–169. https://doi.org/10.1016/0269-7491(91)90031-Q

Grigal, D. F. (2002). Inputs and outputs of mercury from terrestrial watersheds: A review. *Environmental Reviews*, *10*(1), 1–39. https://doi.org/10.1139/a01-013

Grill, G., Lehner, B., Thieme, M., Geenen, B., Tickner, D., Antonelli, F., et al. (2019). Mapping the world's free-flowing rivers. *Nature*, *569*(7755), 215–221. https://doi.org/10.1038/s41586-019-1111-9

Hall, B. D., St. Louis, V. L., Rolfhus, K. R., Bodaly, R. A., Beaty, K. G., Paterson, M. J., & Cherewyk, K. A. P. (2005). Impacts of reservoir creation on the biogeochemical cycling of methyl mercury and total mercury in boreal upland forests. *Ecosystems*, *8*(3), 248–266. https://doi.org/10.1007/s10021-003-0094-3

Hamelin, S., Amyot, M., Barkay, T., Wang, Y., & Planas, D. (2011). Methanogens: Principal methylators of mercury in lake periphyton. *Environmental Science and Technology*, *45*(18), 7693–7700. https://doi.org/10.1021/es2010072

Herrero Ortega, S., Catalán, N., Björn, E., Gröntoft, H., Hilmarsson, T. G., Bertilsson, S., et al. (2018). High methylmercury formation in ponds fueled by fresh humic and algal derived organic matter. *Limnology and Oceanography*, *63*(S1), S44–S53. https://doi.org/10.1002/lno.10722

Hydro-Québec. (2018). Complexe de la Romaine-Bilan des activités environnementales 2017.

James, A. K., Passow, U., Brzezinski, M. A., Parsons, R. J., Trapani, J. N., & Carlson, C. A. (2017). Elevated $pCO_2$ enhances bacterioplankton removal of organic carbon. *PLoS ONE*, *12*(3), e0173145–e0173126. https://doi.org/10.1371/journal.pone.0173145

Jiang, H., Feng, X., & Dai, Q. (2005). Damming effect on the distribution of mercury in Wujiang River. *Chinese Journal of Geochemistry*, *24*(2), 179–183. https://doi.org/10.1007/bf02841163

Kasper, D., Forsberg, B. R., Amaral, J. H. F., Leitão, R. P., Py-Daniel, S. S., Bastos, W. R., & Malm, O. (2014). Reservoir stratification affects methylmercury levels in river water, plankton, and fish downstream from Balbina hydroelectric dam, Amazonas, Brazil. *Environmental Science and Technology*, *48*(2), 1032–1040. https://doi.org/10.1021/es4042644

Kelly, C. A., Rudd, J. W. M., Bodaly, R. A., Roulet, N. P., St. Louis, V. L., Heyes, A., et al. (1997). Increases in fluxes of greenhouse gases and methyl mercury following flooding of an experimental reservoir. *Environmental Science and Technology*, *31*(5), 1334–1344. https://doi.org/10.1021/es9604931

Kelly, C. A., Rudd, J. W. M., St. Louis, V. L., & Heyes, A. (1995). Is total mercury concentration a good predictor of methyl mercury concentration in aquatic systems? *Water, Air, & Soil Pollution.*, *80*(1–4), 715–724. https://doi.org/10.1007/BF01189723

Lapierre, J. F., & Del Giorgio, P. A. (2014). Partial coupling and differential regulation of biologically and photochemically labile dissolved organic carbon across boreal aquatic networks. *Biogeosciences*, *11*(20), 5969–5985. https://doi.org/10.5194/bg-11-5969-2014

Lavoie, R. A., Amyot, M., & Lapierre, J. (2019). Global meta-analysis on the relationship between mercury and dissolved organic carbon in freshwater environments. *Journal of Geophysical Research: Biogeosciences*, *124*, 1508–1523. https://doi.org/10.1029/2018JG004896

Lehner, B., Liermann, C. R., Revenga, C., Vörömsmarty, C., Fekete, B., Crouzet, P., et al. (2011). High-resolution mapping of the world's reservoirs and dams for sustainable river-flow management. *Frontiers in Ecology and the Environment*, *9*(9), 494–502. https://doi.org/10.1890/100125

Lescord, G. L., Emilson, E. J. S., Johnston, T. A., Branfireun, B. A., & Gunn, J. M. (2018). Optical properties of dissolved organic matter and their relation to mercury concentrations in water and biota across a remote freshwater drainage basin. *Environmental Science and Technology*, *52*(6), 3344–3353. https://doi.org/10.1021/acs.est.7b05348

Li, S., Zhou, L., Chang, J., Yang, Z., Hu, J., & Hongjun, W. (2017). The impact of impoundment on mercury bioaccumulation in fish downstream from a newly constructed reservoir, Wujiang River, Southwest China. *Archives of Environmental Contamination and Toxicology*, *73*(4), 570–577. https://doi.org/10.1007/s00244-017-0419-4

Li, S., Zhou, L., Wang, H., Xiong, M., Yang, Z., Hu, J., et al. (2013). Short-term impact of reservoir impoundment on the patterns of mercury distribution in a subtropical aquatic ecosystem, Wujiang River, Southwest China. *Environmental Science and Pollution Research*, *20*(7), 4396–4404. https://doi.org/10.1007/s11356-013-1619-8

Liu, M., Xie, H., He, Y., Zhang, Q., Sun, X., Yu, C., et al. (2019). Sources and transport of methylmercury in the Yangtze River and the impact of the Three Gorges Dam. *Water Research*, *166*, 115042. https://doi.org/10.1016/j.watres.2019.115042

Long, T., Wellen, C., Arhonditsis, G., & Boyd, D. (2014). Evaluation of stormwater and snowmelt inputs, land use and seasonality on nutrient dynamics in the watersheds of Hamilton Harbour, Ontario, Canada. *Journal of Great Lakes Research*, *40*(4), 964–979. https://doi.org/10.1016/j.jglr.2014.09.017

Lucotte, M., Montgomery, S., & Bégin, M. (1999). Mercury dynamics at the flooded soil-water interface in reservoirs of northern Québec: In situ observations. In *Mercury in the biogeochemical cycle* (pp. 165–189). Berlin, Germany: Springer-Verlag. https://doi.org/10.1007/978-3-642-60160-6_9

MacMillan, G. A., Girard, C., Chételat, J., Laurion, I., & Amyot, M. (2015). High methylmercury in Arctic and subarctic ponds is related to nutrient levels in the warming eastern Canadian Arctic. *Environmental Science and Technology*, *49*(13), 7743–7753. https://doi.org/10.1021/acs.est.5b00763

Mailman, M., Stepnuk, L., Cicek, N., & Bodaly, R. A. Drew (2006). Strategies to lower methyl mercury concentrations in hydroelectric reservoirs and lakes: A review. *Science of the Total Environment*, *368*(1), 224–235. https://doi.org/10.1016/j.scitotenv.2005.09.041

Majidzadeh, H., Uzun, H., Ruecker, A., Miller, D., Vernon, J., Zhang, H., et al. (2017). Extreme flooding mobilized dissolved organic matter from coastal forested wetlands. *Biogeochemistry*, *136*(3), 293–309. https://doi.org/10.1007/s10533-017-0394-x

Mason, R., Fitzgerald, W., & Morel, F. (1994). The biogeochemical cycling of elemental mercury: Anthropogenic influences. *Geochimica et Cosmochimica Acta*, *58*(15), 3191–3198. https://doi.org/10.1016/0016-7037(94)90046-9

McCartney, M. (2009). Living with dams: Managing the environmental impacts. *Water Policy*, *11*(SUPPL. 1), 121–139. https://doi.org/10.2166/wp.2009.108

Montgomery, S., Lucotte, M., & Rheault, I. (2000). Temporal and spatial influences of flooding on dissolved mercury in boreal reservoirs. *Science of the Total Environment*, *260*(1–3), 147–157. https://doi.org/10.1016/S0048-9697(00)00559-3

Mucci, A., Montgomery, S., Lucotte, M., Plourde, Y., Pichet, P., & van Tra, H. (2008). Mercury remobilization from flooded soils in a hydroelectric reservoir of northern Quebec, La Grande-2: Results of a soil resuspension experiment. *Canadian Journal of Fisheries and Aquatic Sciences*, *52*(11), 2507–2517. https://doi.org/10.1139/f95-841

Murphy, K. R., Butler, K. D., Spencer, R. G. M., Stedmon, C. A., Boehme, J. R., & Aiken, G. R. (2010). Measurement of dissolved organic matter fluorescence in aquatic environments: An interlaboratory comparison. *Environmental Science and Technology*, *44*(24), 9405–9412. https://doi.org/10.1021/es102362t

Pakhomova, S. V., Hall, P. O. J., Kononets, M. Y., Rozanov, A. G., Tengberg, A., & Vershinin, A. V. (2007). Fluxes of iron and manganese across the sediment-water interface under various redox conditions. *Marine Chemistry*, *107*(3), 319–331. https://doi.org/10.1016/j.marchem.2007.06.001

Paranjape, A. R., & Hall, B. D. (2017). Recent advances in the study of mercury methylation in aquatic systems. *Facets*, *2*(1), 85–119. https://doi.org/10.1139/facets-2016-0027

Poff, N. L., & Hart, D. D. (2002). How dams vary and why it matters for the emerging science of dam removal. *Bioscience*, *52*(8), 659–668. https://doi.org/10.1641/0006-3568(2002)052[0659:hdvawi]2.0.co;2

Quémerais, B., Cossa, D., Rondeau, B., Pham, T. T., & Fortin, B. (1998). Mercury distribution in relation to iron and manganese in the waters of the St. Lawrence River. *Science of the Total Environment*, *213*(1–3), 193–201. https://doi.org/10.1016/S0048-9697(98)00092-8

Roy, V., Amyot, M., & Carignan, R. (2009). Beaver ponds increase methylmercury concentrations in Canadian shield streams along vegetation and pond-age gradients. *Environmental Science and Technology*, *43*(15), 5605–5611. https://doi.org/10.1021/es901193x

St. Louis, V. L., Rudd, J. W. M., Kelly, C. A., Beaty, K. G., Bloom, N. S., & Flett, R. J. (1994). Importance of wetlands as sources of methyl mercury to boreal forest ecosystems. *Canadian Journal of Fisheries and Aquatic Sciences*, *51*(5), 1065–1076. https://doi.org/10.1139/f94-106

St. Louis, V. L., Rudd, J. W. M., Kelly, C. A., Bodaly, R. A., Paterson, M. J., Beaty, K. G., et al. (2004). The rise and fall of mercury methylation in an experimental reservoir. *Environmental Science and Technology*, *38*(5), 1348–1358. https://doi.org/10.1021/es034424f

Teodoru, C. R., Bastien, J., Bonneville, M. C., Del Giorgio, P. A., Demarty, M., Garneau, M., et al. (2012). The net carbon footprint of a newly created boreal hydroelectric reservoir. *Global Biogeochemical Cycles*, *26*, GB2016. https://doi.org/10.1029/2011GB004187

U.S. Environmental Protection Agency (2001). *Method 1630, methyl mercury in water by distillation, aqueous ethylation, purge and trap, and cold-vapor atomic fluorescence spectrometry*. Washington, DC: U.S. Environmental Protection Agency.

U.S. Environmental Protection Agency (2002). *Method 1631: Mercury in water by oxidation, purge and trap, and cold vapor atomic fluorescence spectrometry*. Washington, DC: U.S. Environmental Protection Agency.

Ullrich, S. M., Tanton, T. W., & Abdrashitova, S. A. (2001). Mercury in the aquatic environment: A review of factors affecting methylation. *Critical Reviews in Environmental Science and Technology*, *31*(3), 241–293. https://doi.org/10.1080/20016491089226

Wang, F., & Zhang, J. Z. (2013). Mercury contamination in aquatic ecosystems under a changing environment: Implications for the Three Gorges Reservoir. *Chinese Science Bulletin*, *58*(2), 141–149. https://doi.org/10.1007/s11434-012-5490-7

Wünsch, U. J., Bro, R., Stedmon, C. A., Wenig, P., & Murphy, K. R. (2019). Emerging patterns in the global distribution of dissolved organic matter fluorescence. *Analytical Methods*, *11*(7), 888–893. https://doi.org/10.1039/c8ay02422g

Zhao, L., Guo, Y., Meng, B., Yao, H., & Feng, X. (2017). Effects of damming on the distribution and methylation of mercury in Wujiang River, Southwest China. *Chemosphere*, *185*, 780–788. https://doi.org/10.1016/j.chemosphere.2017.07.077

Zhou, T., Nijssen, B., Gao, H., & Lettenmaier, D. P. (2015). The contribution of reservoirs to global land surface water storage variations. *Journal of Hydrometeorology*, *17*(1), 309–325. https://doi.org/10.1175/jhm-d-15-0002.1